

OPTICS MEASUREMENTS AT SUPERKEKB USING BEAM BASED CALIBRATION FOR BPM AND BBA

Hiroshi Sugimoto*, Yuki Yoshi Ohnishi, Haruyo Koiso, Akio Morita, Kenji Mori, Masaki Tejima
 KEK, Tsukuba, Japan

Abstract

The beam-based calibration (BBC) technique for Beam-Position-Monitor (BPM) is applied in order to establish reliable optics measurement in SuperKEKB. A response model between beam position, charge and output signals of the BPM electrodes are introduced to calibrate the relative gain of the BPM electrodes (BPM Gain Calibration, BGC). The gains are adjusted by total squares fitting so that the model reproduces the measured BPM signals. The Beam-Based Alignment (BBA) is also performed to determine the magnetic center of a quadrupole. Using BGC and BBA, the performance of the BPM system and optics correction are successfully improved. This talk presents what we experienced in SuperKEKB so far focusing on beam optics measurement and some details on the beam-based calibration scheme for BPM system.

INTRODUCTION

SuperKEKB [1] is an electron-positron double ring collider and aiming to open up new luminosity frontier. The target peak luminosity of $8 \times 10^{35} \text{cm}^{-2}\text{s}^{-1}$ is 40 times higher than that achieved by the preceding project, KEKB [2]. SuperKEKB consists of electron (HER) and positron (LER) storage rings with an injector linac and a newly constructed positron damping ring. The design concept is based on the nano-beam scheme [3], in which both beams are squeezed to nano-scale sizes and collided with a larger crossing angle at the interaction point (IP). The key changes of machine parameters from KEKB are 2 times higher beam current, 1/20 times smaller vertical betatron function at the (IP). Low emittance tuning (LET) is essential for the nano-beam scheme as well as squeezing the betatron function.

The SuperKEKB commissioning has started in 2016 after over 5 years of the upgrade work. The initial beam commissioning named Phase 1 [4] started on 1st February 2016 and finished on 28th June 2016. The final focusing quadrupole magnets (QCSs) for beam collision is not installed in Phase 1. The Phase 1 operation was devoted to the vacuum scrubbing and the basic setup of operating system. After installation of QCSs, the second beam commissioning (Phase 2) started on 19th March 2018 and finished on 17th July 2018 [5]. The first beam collision was observed at 26th April 2018. The 3rd beam commissioning phase (Phase 3) is started on 11th March 2019 [6].

Calibration of the BPM system is a key issue for better control of beam orbit and optics. We employ the BBC technique to the BPM system as at KEKB [7]. In BBC, both the relative gain of the BPM electrodes and the relative offset

* hiroshi.sugimoto@kek.jp

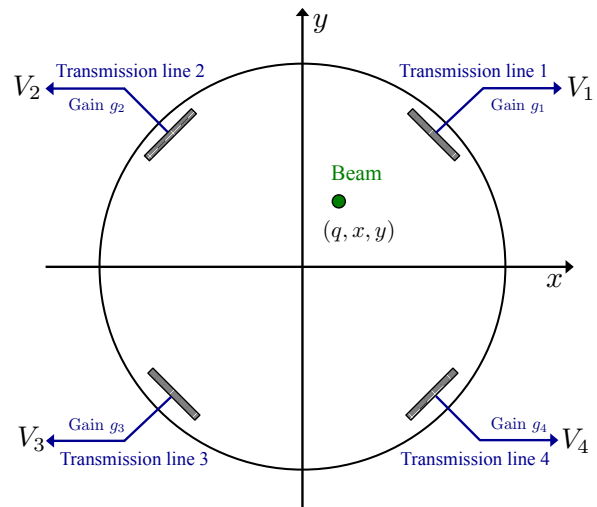


Figure 1: Schematic view of the BPM model used in BGC.

between the BPM electrical center and the magnetic center of a quadrupole are determined using measured BPM signals. In this paper we show the idea and results of BBC together with experience on the LET in Phase 1 and 2.

BPM SYSTEM

The SuperKEKB main rings have about 900 quadrupole magnets, and BPM is attached to all quadrupole magnets for precise orbit control. Most of the BPMs installed in the HER are based on 1 GHz narrow-band system [8] reused from KEKB since most of the vacuum chambers are same as those of KEKB. On the other hand, the vacuum chambers of LER are replaced with new ones with ante-chamber structure, and the waveguide cutoff frequency of the chamber is lower than 1 GHz in SuperKEKB. Therefore a newly developed narrow-band system is installed in the LER.

The BPM system is successfully used in the beam tuning with an averaging mode of 0.25 Hz. In addition to closed-orbit measurement, more than 100 BPMs can be used as gated turn-by-turn BPMs. The gated turn-by-turn BPM system is very helpful in injection tuning. Although optics measurement with turn-by-turn beam position data is applied, we concentrate on the BBC and beam measurement based on closed-orbit analysis in this paper.

BEAM-BASED CALIBRATION

Two calibration factors are discussed here. One is calibration of relative gains of the BPM electrodes and the other is the determination of the BPM offset relative to the neighbour

Content from this work may be used under the terms of the CC BY 3.0 licence (© 2019). Any distribution of this work must maintain attribution to the author(s), title of the work, publisher, and DOI

quadrupole magnet. In this section, we show a strategy of these calibration work and its result.

BPM Gain Calibration

In the presented BPM system, a BPM has four button-type pickups and outputs four voltages $V_{1,2,3,4}$ induced by the beam as shown in Fig. 1. In order to eliminate dependency on beam intensity, normalized horizontal and vertical voltages (u, v) are introduced as,

$$u \equiv (V_1 - V_2 - V_3 + V_4) / \Sigma, \quad (1)$$

$$v \equiv (V_1 + V_2 - V_3 - V_4) / \Sigma, \quad (2)$$

where Σ is the sum of all four voltages. These normalized variables are transformed to horizontal and vertical beam positions (x, y) by using mapping functions as $x = F_x(u, v)$ and $y = F_y(u, v)$. The functions $F_{x,y}(u, v)$ are approximated by third order polynomial functions. The polynomial coefficients are obtained numerically by a finite boundary element method with a two-dimensional electrostatics BPM model.

Assuming the ideal BPM with a perfectly conducting beam pipe and considering the transverse electric and magnetic field, the output voltage of i -th electrode is expressed by a single response function $F_i(x, y)$ as $V_i = qF_i(x, y)$. The voltage of each electrode is measured through a detector system after traveling through a different transmission path. Therefore the response of each electrode also depends on the electrical characteristic of the transmission path and may be different from that of the ideal system.

We introduce a single calibration factor g_i to i -th electrode, called its gain, in order to describe the imbalance among the electrical characteristics of the four electrodes. The measured voltage is now re-written as $V_i = g_i q F_i(x, y)$, and all gains are equal to 1 for the ideal condition. Because only the relative value is essential in the beam positions evaluation, we choose $g_1 = 1$ in the following.

The gain factor is determined by a beam measurement so that the BPM model reproduces the measured BPM signals [9]. For this purpose we minimize a chi-square function,

$$\chi^2 \equiv \sum_i^4 \sum_j^m \frac{[V_{ij} - g_i q_j F(x_i, y_i)]^2}{\sigma_{ij}^2}, \quad (3)$$

where V_{ij} is the j -th measured voltage of the i -th electrode and m is the number of measurements. The fitting parameters are three gain factors $g_{2,3,4}$, m sets of beam charges and positions (q_j, x_j, y_j). Therefore the problem to be solved is finding $3 + 3m$ unknown parameters from $4m$ measured voltages. It is expected that the unique solution can be obtained when the number of fitting variables becomes larger than that of measurement data, that is, $m > 4$. A sufficiently wide area of beam position data is essential to avoid degeneracy of the measurement data and failure in the chi-square minimization.

The response function $F_i(x, y)$ is approximated by a fourth order polynomial fit to numerical data obtained with the BPM model. The Levenberg-Marquardt algorithm [10, 11]

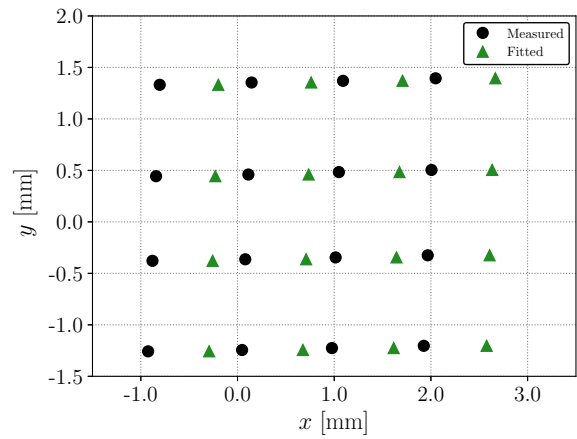


Figure 2: Example of the gain calibration. The dots represent measured beam position before the fitting, while the triangles represent beam positions obtained by the chi-square minimization.

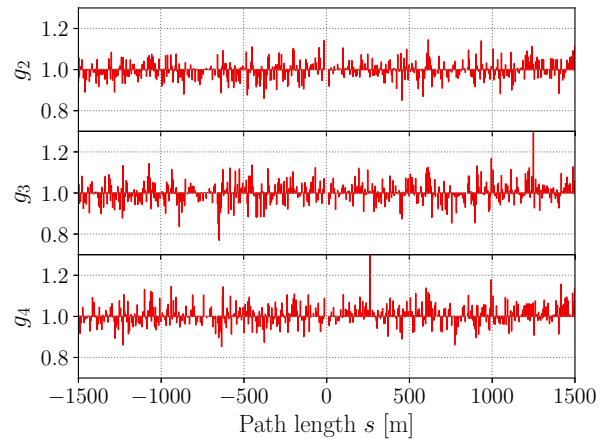


Figure 3: Gain parameters for the LER BPMs.

is employed to minimizing χ^2 . The BPM reading and gain factors at that point is chosen as an initial guess of the unknown parameters in the optimization algorithm.

Figure 2 illustrates experimental result obtained in the LER, where beam positions before the BGC and those obtained by the chi-square minimization are shown. The electrode voltages are measured while changing strength of horizontal and vertical steering magnets. The chi-square χ^2 defined in Eq. (3) is converged from after 17 numerical iterations, and the resultant gains are $(g_2, g_3, g_4) = (0.994, 1.031, 0.987)$.

The BGC is performed for all BPMs in the both LER and HER. The obtained gain factors of the LER BPMs are plotted along the ring in Fig. 3. The deviation from the ideal gain $\Delta g_{2,3,4} \equiv g_{2,3,4} - 1$ is about 5% in the root-mean-square.

Beam position is normally evaluated by using all four electrodes. It is also possible to calculate beam position by only using three electrodes among four electrodes. Therefore four beam positions $z_{a,b,c,d}$ are obtained by changing combination of electrodes, where z stands for x or y . These

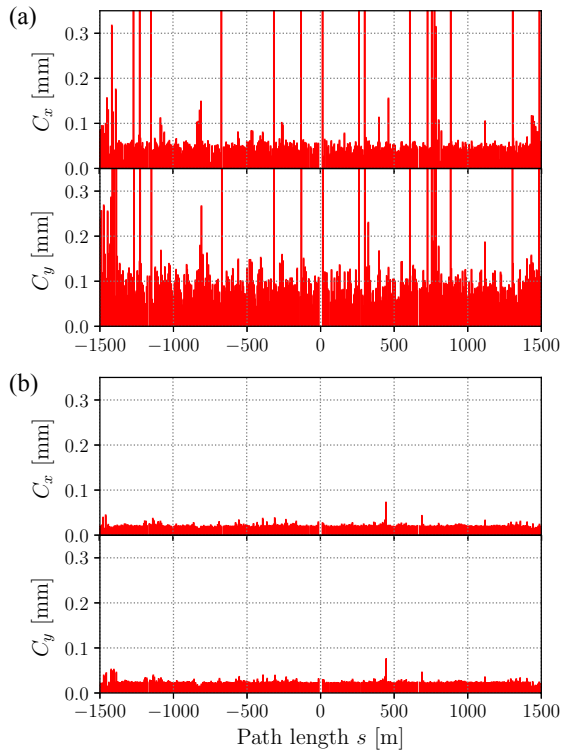


Figure 4: Consistency error of BPMs in the LER (a) before and (b) after BGC.

four positions coincide each other in the ideal system. The validity of BGC and the soundness of the BPM system are evaluated by the standard deviation of $z_{a,b,c,d}$ as,

$$C_z \equiv \sqrt{\frac{1}{4} \sum_{i=a,b,c,d} (z_i - \langle z \rangle)^2}, \quad \langle z \rangle \equiv \frac{1}{4} \sum_{i=a,b,c,d} z_i, \quad (4)$$

and $C_z = 0$ for the ideal condition. We call the parameter C_z as the consistency error of the BPM.

Figure 4 shows the consistency error before and after BGC in the LER. The consistency is remarkably improved by the presented calibration technique. The consistency error is routinely monitored during beam operation to detect a hardware trouble in the BPM system.

Beam Based Alignment

Another calibration parameter discussed in this paper is the BPM offset, that is, a misalignment between the magnetic center of a neighbour quadrupole magnet and the BPM electrical center. The BPM offset respect to the magnet causes unexpected orbit and optics distortion and may lead emittance degradation.

The offset respect to an adjoined quadrupole magnet is determined by Beam-Based-Alignment (BBA) technique [12]. We find a BPM reading which is insensitive to the field gradient of the quadrupole magnet as shown in Fig. 5. Response of beam position (x, y) respect to the field gradient K_1 is measured for three kinds of closed orbits. Linear fitting is

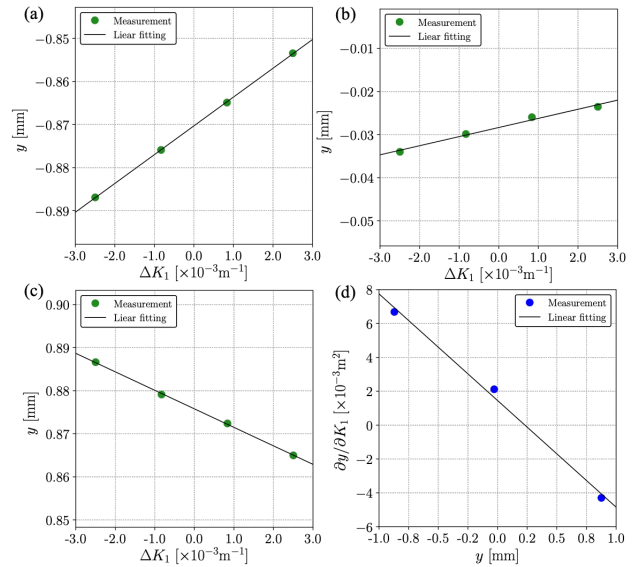


Figure 5: Example of BBA. Beam positions y as a function of the field gradient of adjoined quadrupole magnet K_1 for three kinds of closed orbits are shown in (a), (b) and (c). Orbit response $\partial y / \partial K_1$ as a function of the BPM reading is shown in (d).

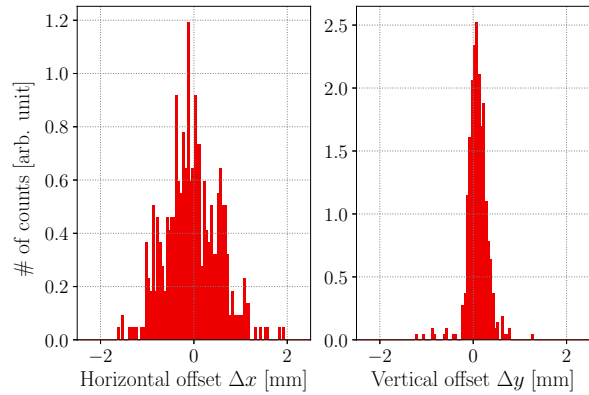


Figure 6: Offset distribution for the LER BPMs.

applied to the measured data to find a BPM reading at which $\partial x, y / \partial K_1 = 0$. The measurement is performed by using a semi-automated software implemented by the accelerator code SAD [13]. The obtained offset information is incorporated into the BPM system. The offset distributions in the LER BPMs is shown in Fig. 6. The horizontal offset is somehow larger than the vertical offset. It is conformed that the BPM offset in the HER BPMs shows the same tendency. This result is likely owing to the mounting structure of BPM and its installation process. The magnet have a stand for BPM installation, and the BPM is bolted on the stand. The bolt diameter is somewhat smaller than hole diameter for adjustment margin in the installation. Prior mechanical alignment work is omitted to save construction time. Conse-

Content from this work may be used under the terms of the CC BY 3.0 licence (© 2019). Any distribution of this work must maintain attribution to the author(s), title of the work, publisher, and DOI

quently, the horizontal misalignment is larger than that of vertical direction.

OPTICS MEASUREMENT AND CORRECTION

The beam optics is measured by analyzing closed-orbit distortions induced by dipole kicks to the beam or frequency change of rf cavities. The important optics parameters in the LET are the vertical dispersion function and the coupling between horizontal and vertical betatron motions (xy -coupling parameter). The xy -coupling parameter is a correlation between horizontal and vertical betatron motions, thus a vertical leakage orbit caused by a horizontal dipole kick reflects xy -coupling parameters. Six kinds of vertical leakage orbits are measured by using six different steering magnets considering the betatron phase advance among them. The correction of xy -coupling is performed against these leakage orbits. Measured leakage orbits and vertical dispersion are suppressed by using skew quadrupole correctors which are newly installed to sextupole magnets in SuperKEKB. The adjustment of the skew quadrupole field is calculated with the measured optics and the model response matrix computed by SAD. The performance of the optics correction in Phase 1 and 2 is summarized in Table 1, where root-mean-square residual of vertical leakage orbit $\Delta y^{\text{rms}}/\Delta x^{\text{rms}}$, dispersion $\Delta\eta_{x,y}^{\text{rms}}$ and betatron function $(\Delta\beta_{x,y}/\beta_{x,y})^{\text{rms}}$ is evaluated.

Table 1: Summary of Optics Correction in Phase 1 and 2

Items	Phase 1		Phase 2	
	LER	HER	LER	HER
$\Delta y^{\text{rms}}/\Delta x^{\text{rms}} [10^{-3}]$	9	6	14	8
$\Delta\eta_x^{\text{rms}} [\text{mm}]$	8	11	10	9
$\Delta\eta_y^{\text{rms}} [\text{mm}]$	2	2	4	3
$(\Delta\beta_x/\beta_x)^{\text{rms}} [\%]$	3	3	2	3
$(\Delta\beta_y/\beta_y)^{\text{rms}} [\%]$	3	3	4	3

Phase 1 Operation

The vertical leakage orbits in the LER measured before and after the xy -coupling correction are shown in Figs. 7(a) and 7(b), respectively. After adjusting the skew quadrupole correctors, the vertical leakages are significantly suppressed. However, an uncorrectable leakage orbit was observed around $s = -1300$ m.

We find after a series of investigations that the uncorrectable xy -coupling is due to the leakage field from a Lambertson septum magnet which delivers aborted beams to a beam dump. Two cures are applied during Phase 1. One is activation of skew quadrupole coils installed in the nearby sextupole magnets by using spare power supplies. Another cure is installation of permanent magnets. We attached ferrite magnets with field strength of 0.07 T to the beam chamber near the septum magnet [14]. The xy -coupling due to the leakage field is successfully reduced by these cures as

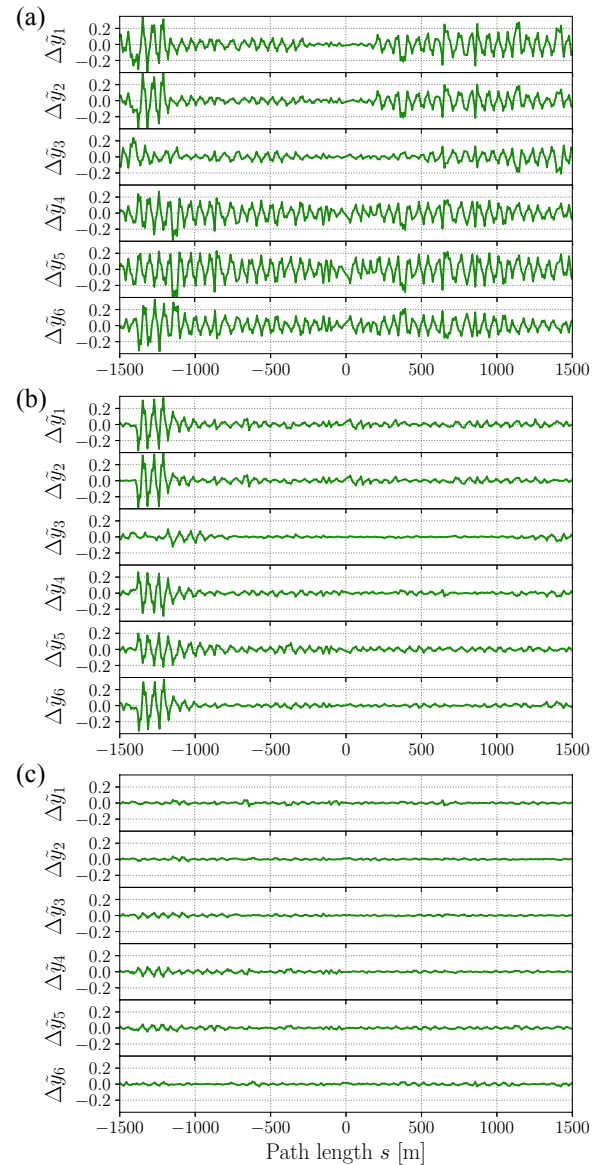


Figure 7: Measured vertical leakage orbits induced by horizontal dipole kicks in the LER ring (a) before correction, (b) after correction, (c) after two countermeasures for the leakage field of the Lambertson septum magnet. The vertical axis is normalized by root-mean-square amplitudes of the horizontal orbit.

shown in Fig. 7(c). The same problem is observed in the HER, and we applied same cures.

The achieved lowest vertical emittance of the LER beam is about 10 pm according to vertical beam size measured by a X-ray beam size monitor. This value is consistent with that estimated by measured beam optics. On the other hand the vertical emittance of the HER beam is about 40 pm. It is considerably larger than 10 pm expected from measured beam optics. One difference between the LER and the HER in beam size measurement is the vertical betatron function at the X-ray source point β_y^s . The betatron function

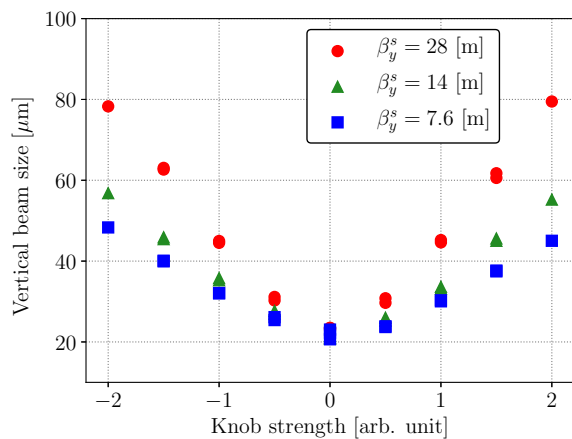


Figure 8: Vertical beam size of the electron beam as a function of strength of vertical dispersion knob with three different betatron functions at the X-ray source point β_y^s .

is $\beta_y^s = 67$ m in the LER, whereas $\beta_y^s = 8$ m in the HER. Therefore, the required resolution is higher in the HER when the emittance is comparable in the both rings.

Phase 2 Operation

Several new types of equipment were installed to X-ray extraction to improve the resolution of the beam size measurement [15]. In addition to the monitor upgrade, some pole changers are installed to quadrupole magnets in the HER to enlarge β_y^s .

Beam size measurement in the HER with three different β_y^s is performed to investigate dependency of the measured beam size on β_y^s . Vertical beam size is measured while changing vertical dispersion along the ring. Some of skew quadrupole correctors are used as a control knob for vertical dispersion. The measurement results are summarized in Fig. 8, where measured vertical beam size with the strength of the vertical-dispersion knob is shown. The measured vertical beam size becomes less sensitive to the vertical-dispersion knob when β_y^s becomes smaller. The minimum measured beam size is, however, independent on β_y^s . This observation implies that the measurement system has smearing effects which limit the measurement resolution. More comprehensive study estimates that the size of smearing effect is about $6 \mu\text{m}$ [15]. The smallest vertical beam size in the HER observed so far is $16 \mu\text{m}$ in including the smearing effect. It is presumed with the smearing effect of $6 \mu\text{m}$ that the achieved vertical emittance of the HER beam is 8 pm .

The achieved lowest vertical emittance of the LER beam is 23 pm and is larger than that in Phase 1. The residual xy -coupling is indeed larger than that in Phase 1 as shown in Table 1. The reason for the degradation is not fully understood, and we have a plan to perform BBA again and examine the closed orbit more carefully.

CONCLUSION

The BBC technique for the BPM system in the SuperKEKB operation and the results of the LET are presented.

Assuming the BPM model, the relative gains of the BPM electrodes are calibrated so that the model reproduces the measured output voltages. The BPM offset respect to the magnetic center of the neighbour quadrupole magnet is determined by finding the BPM reading which is insensitive to the quadrupole field gradient.

The optics correction using the reliable BPM system is successfully worked. The vertical emittance of 10 pm is achieved in LER during the Phase 1 operation. The achieved emittance of the LER beam in Phase 2 is 23 pm and is larger than that in Phase 1. The reason for the degradation is still under investigation. The beam size monitor in the HER shows smearing effects which limit the measurement resolution. It is presumed that the achieved vertical emittance of the HER beam is 8 pm .

ACKNOWLEDGEMENTS

The authors would like to thank the entire SuperKEKB accelerator group for developing the hardware system and supporting the beam measurement presented in this paper.

REFERENCES

- [1] Y. Ohnishi *et al.*, Prog. Theor. Exp. Phys. 2013 03A011 (2013).
- [2] T. Abe *et al.*, Prog. Theor. Exp. Phys. 2013 03A001 (2013).
- [3] C. P. Raimondi, 2nd SuperB Workshop, Frascati, Italy, Mar. 16-18, 2006.
- [4] Y. Funakoshi *et al.*, in Proc. of IPAC'16, Busan (Korea, 2016), pp. 1019-1021.
- [5] Y. Ohnishi *et al.*, in Proc. of IPAC'18, Vancouver (Canada, 2018), pp. 1-5.
- [6] A. Morita *et al.*, "Status of Early SuperKEKB Phase-3 Commissioning", presented at the 10th International Particle Accelerator Conf. (IPAC'19), Melbourne, Australia, May. 2019, paper WEYYPLM1, this conference.
- [7] M. Tejima, in Proc. of IBIC2015, Melbourne (Australia, 2015) pp. 267-272.
- [8] M. Arinaga *et al.*, Prog. Theor. Exp. Phys. 2013 03A007 (2013).
- [9] K. Satoh and M. Tejima, in Proc. of PAC1997, Vancouver (Canada, 1997), pp. 2087-2089.
- [10] D. Marquardt, J. Soc. Indus. Appl. Math., Vol. 11, no 2, pp. 431-441, June 1963.
- [11] H.B. Nielsen, Technical Report, IMM-REP-1999-05, Technical University of Denmark, 1999.
- [12] M. Masuzawa *et al.*, in Proc. of EPAC2000, Vienna (Austria, 2000), pp. 1780-1782.
- [13] K. Oide, Nucl. Inst. Meth. A 276, 427 (1989). <http://acc-physics.kek.jp/SAD/>
- [14] N. Iida *et al.*, in Proc. of IPAC2017, Copenhagen (Denmark, 2017) pp. 2918-2921.
- [15] E. Mulyani, Nucl. Inst. Meth. A 919, 1 (2019).